



Structural optimization towards promising β -methyl-4-acrylamido quinoline derivatives as PI3K/mTOR dual inhibitors for anti-cancer therapy: The *in vitro* and *in vivo* biological evaluation



Ruoyu He ^{a, b, 1}, Bingyong Xu ^{b, c, 1}, Li Ping ^d, Xiaoqing Lv ^{b, *}

^a Department of Pharmaceutical Preparation, Hangzhou Xixi Hospital, Hangzhou, 310023, China

^b College of Medicine, Jiaying University, Jiaying, 314001, China

^c Zhejiang Heze Pharmaceutical Technology Co., LTD, Hangzhou, 310018, China

^d Center for Drug Safety Evaluation and Research, College of Pharmaceutical Sciences, Zhejiang University, Hangzhou, 310058, China

ARTICLE INFO

Article history:

Received 20 October 2020

Received in revised form

24 January 2021

Accepted 25 January 2021

Available online 1 February 2021

Keywords:

PI3K

mTOR

Cancer

PI3K/mTOR dual inhibitor

Quinoline derivatives

ABSTRACT

Built upon the 4-acrylamido quinoline derivative **4**, a previously discovered PI3K/mTOR dual inhibitor, structural modification was undertaken in this study with the attempt to improve its oral exposure via introducing steric hindrance to the 4-acrylamido functionality. Consequently, **14d**, as the representative among the synthesized compounds, exhibited IC₅₀ values of 0.80, 0.67, 1.30, 1.30 and 5.0 nM against PI3K α , PI3K β , PI3K γ , PI3K δ and mTOR, respectively. Besides, **14d** displayed comparable anti-proliferative activity against both PC3 and U87MG cell lines to that of the positive reference GSK2126458 with respective GI₅₀ value of 0.36 and 0.14 μ M. Kinase selectivity assay showed that **14d** was selective to PI3K family. In U87MG cells, **14d** can strongly down-regulate PI3K/Akt/mTOR pathway via blocking both PI3K and mTOR signaling at the concentration as low as 25 nM. Importantly, following a PO dose of 5 mg/kg in male SD rats, **14d** displayed favorable oral exposure (AUC_{0-t} = 1336.16 h \times ng/mL, AUC_{0- ∞} = 1447.63 h \times ng/mL) and high maximum plasma concentration (C_{max} = 903.00 ng/mL). In a U87MG glioblastoma xenograft model, tumor growth inhibition of 93.5% and tumor regression were observed at PO dose of 30 and 60 mg/kg, respectively. Meanwhile, no overt loss of body weight was observed in the **14d**-treated groups. Taken together, **14d**, by virtue of its attractive performance, merits further development as a potential anti-tumor candidate.

© 2021 Elsevier Masson SAS. All rights reserved.

1. Introduction

Phosphoinositide 3-kinase/Akt/mammalian target of rapamycin (PI3K/Akt/mTOR, PAM) pathway has attracted massive pharmaceutical investments in exploring its inhibitors for battling human malignancies [1–3]. PI3K, the upstream effector along the pathway, comprises three classes, known as class I, class II, and class III PI3Ks. Owing to the differentiation in catalytic subunit and biological function, class I PI3Ks are further divided into four isoforms, termed as PI3K α , β , γ , and δ . In particular, PI3K α and β have been identified to be drivers in a myriad of cancers. Besides, PI3K δ has been verified to be closely relevant to leukocyte-mediated malignancies [4].

mTOR, the downstream signaling effector along PAM cascade,

belongs to the phosphatidylinositol 3-kinase-related kinase family. Both PI3K and mTOR are attractive anti-cancer targets with great medicinal potential, as testified by the clinical advancement of numerous inhibitors targeting PI3K or (and) mTOR [5]. As for selective PI3K inhibitors, alpelisib (PI3K α inhibitor), idelalisib (PI3K δ subtype-selective inhibitor), copanlisib (PI3K α/δ dual inhibitor) and duvelisib (PI3K γ/δ dual inhibitor) have been successively approved for the treatment of leukocyte-mediated malignancies [6–9]. Everolimus, sirolimus and temsirolimus are all mTOR allosterically inhibitors. As for indications, everolimus has been approved for prevention of allograft rejection, treatment of cancer and TSC-associated seizures; sirolimus is used for prevention of allograft rejection; temsirolimus is used as anti-cancer agent [10–12]. Recently, numbers of ATP competitive mTOR-selective inhibitors showed promising anti-cancer efficacy, such as CC-223, INK128, AZD2014, PQR620, and tricyclic pyrimido-pyrrolo-oxazines [13–17]. In addition, ATP competitive mTOR-selective inhibitors

* Corresponding author.

E-mail address: lxqd1@zju.edu.cn (X. Lv).

¹ These authors contributed equally to this work.

have been very recently explored in preclinical development for neurological disorders and epilepsy, such as PQR626, and thiazopyrimidines [18,19].

The compromised response to kinase inhibitors (KIs) induced by intrinsic drug resistance mechanisms has emerged as a major concern of research community [20,21]. Among these, the augmented downstream signaling is frequently observed. Persistently active mTOR signaling is sufficient for limiting the sensitivity to PI3K inhibitor, and the reactivation of mTOR signaling has been observed in tumors from patients whose disease progressed after treatment solely targeting PI3K [22]. Moreover, the clinical application of mTOR allosteric modulators is hindered by the release of S6K/IRS1/PI3K negative feedback loop, which activates PI3K and neutralizes the therapeutic efficacy resulted from mTOR inhibition [23,24]. In view of these, dual inhibition of PI3K and the downstream effector mTOR with a single drug molecule is beneficial for surmounting or delaying these resistance mechanisms, in addition to conferring a two-spot ablation of PAM pathway and producing a synergism. In addition, due to the homology of mTOR to PI3K in the catalytic region, a number of PI3K inhibitors concomitantly inactivate mTOR. So far, numerous PI3K/mTOR dual inhibitors have been progressed into clinical investigation, such as BEZ235 (1), BGT226 (2), GSK2126458 (3), GDC-9080, PF-04691502, PQR309, and recently discovered inhibitors PQR514 and PQR530 [25–32]. Among them, BEZ235 (1), BGT226 (2), GSK2126458 (3) share the quinoline template, which serves as an ideal H-bond acceptor to confer interaction with the hinge region of both PI3K and mTOR (Fig. 1).

During our pursuit of quinoline-based PI3K/mTOR dual inhibitors, a novel series of 4-acrylamido derivatives has been discovered *via* probing amino acid residue located at the entrance to ATP-binding pocket of PI3K. The representative compound **4** showed strong potency *in vitro* but with low oral exposure *in vivo* (379 h × ng/mL following the oral gavage at the dosage of 5 mg/kg in male Sprague-Dawley (SD) rats), which needs further structural modifications to improve its pharmacokinetic (PK) properties (Fig. 2) [33]. In respect of the chemical structure of **4**, the existence of 4-acrylamido functionality, it is probable that the Michael-acceptor can be captured *in vivo*, may be responsible for lowering the oral exposure. Hence, our strategy to optimize **4** prioritized introduction of steric hindrance by replacing the β -H of the 4-acrylamido functionality with a methyl group. Besides, the *E* or *Z*-configuration was investigated for a more favorable binding affinity, and several terminal amine groups of the 4-acrylamido functionality were introduced for modifying the physicochemical properties. Above all, we herein communicate our approach to attaining potent 4-acrylamido-quinoline-derived PI3K/mTOR dual inhibitors with improved oral exposure, as well as favorable *in vitro* and *in vivo* potency.

2. Results and discussion

2.1. Chemistry

The synthetic route for β -methyl-4-acrylamido-quinolines **14a–f** is outlined in Scheme 1. Reaction of 4-bromoaniline **5** with methyl vinyl ketone in the presence of FeCl₃ and ZnCl₂ provided 4-methyl-6-bromoquinoline **6**. Following oxidation of **6** with SeO₂, the newly formed 6-bromoquinoline-4-carbaldehyde **7** was treated with MeMgBr, thereby leading to the generation of quinolin derivative **8**. Afterwards, oxidation of **8** with Dess-Martin afforded 1-(5-bromoquinolin-4-yl)ethan-1-one **9**, which was treated with triethyl phosphonoacetate to give the intermediates ethyl (*E*)-3-(5-bromoquinolin-4-yl)but-2-enoate **10a** and ethyl (*Z*)-3-(5-bromoquinolin-4-yl)but-2-enoate **10b**. The configuration (*E/Z*) of

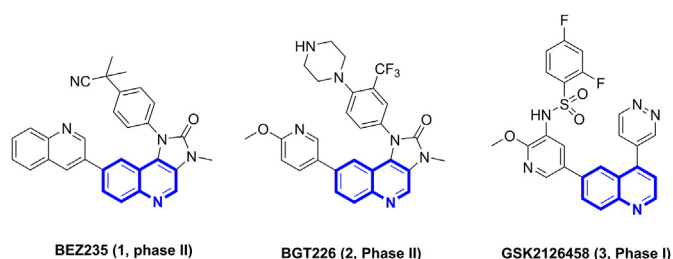


Fig. 1. Clinically investigated PI3K/mTOR dual inhibitors bearing quinoline as the hinge binder.

10a or **10b** was determined by Nuclear Overhauser Effect (NOE, data provided in the supplemental material). As shown in Scheme 1, NOE correlations of H-2'/H-3 and H-2'/H-4' were observed in **10a**, which suggested the configuration of the carbon-carbon double bond was *E*. On the contrary, NOE correlations of H-2'/H-3, and H-2'/H-4' were not observed in **10b**, thereby indicating the *Z* configuration of the carbon-carbon double bond.

Subsequently, **10a** and **10b** through hydrolysis, condensation and Suzuki coupling with the borate **13** afforded the target compounds **14a–f**, respectively.

2.2. Enzymatic activity against PI3K α and mTOR

Given the important role played by abnormal PI3K α signaling in cancer, all the target compounds were first assayed for their inhibitory activities against PI3K α with the clinically investigated GSK2126458 as the positive reference (Table 1). As a result, a majority of them (**14a–e**) exhibited single-digit nanomolar or subnanomolar inhibitory activities against PI3K α . In the mTOR inhibitory activity assay, **14a–e** also showed favorable inhibitory activity with IC₅₀ values below 10 nM. Among these compounds, **14d** exerted the most potent inhibitory activity against PI3K α with IC₅₀ value of 0.80 nM, which was comparable to that of GSK2126458.

As for the structure-activity relationship (SAR), it was consistent with our previous docking analysis [24]. As exemplified by the modeling of **14c** docking into the ATP-binding pocket of PI3K α (PDB code 4JPS), which showed that *E*-configuration acrylamide on **14c** form an additional hydrogen bond with Gln 859, leading to the approximately 21-fold enhancement in PI3K α inhibitory activity compared to *Z*-configuration compound **14f** (Fig. 3). Hence, the *E*-configuration of the C=C double bond was more beneficial for enzymatic activity.

2.3. Anti-proliferative activity

Consistent with their potent enzymatic activity, compounds **14a–e** displayed remarkable cytotoxic activities against both prostate cancer PC3 and glioblastoma U87MG cell lines with GI₅₀ values at low micromolar or submicromolar level (Table 1). Throughout these, the anti-proliferative activity of **14a** and **14d** against both cell lines was comparable to that of GSK2126458 with the GI₅₀ values below 0.5 μ M. In particular, compound **14d** exerted the most attractive activity against U87MG cell line with GI₅₀ value of 0.14 μ M.

2.4. Enzymatic activity against other class I PI3Ks

Owing to its most potent PI3K α inhibitory activity throughout this series and the attractive anti-proliferative activity, **14d** was selected for evaluating the potency against other class I PI3K

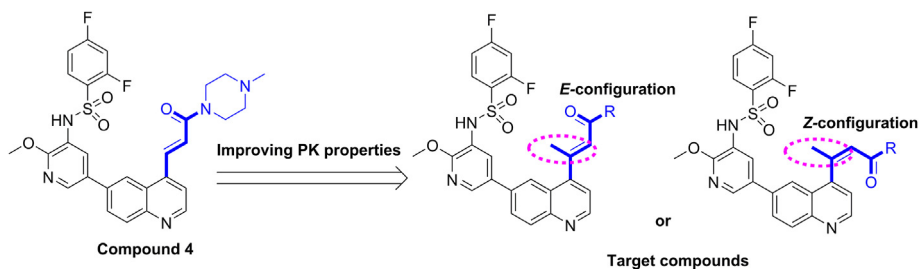
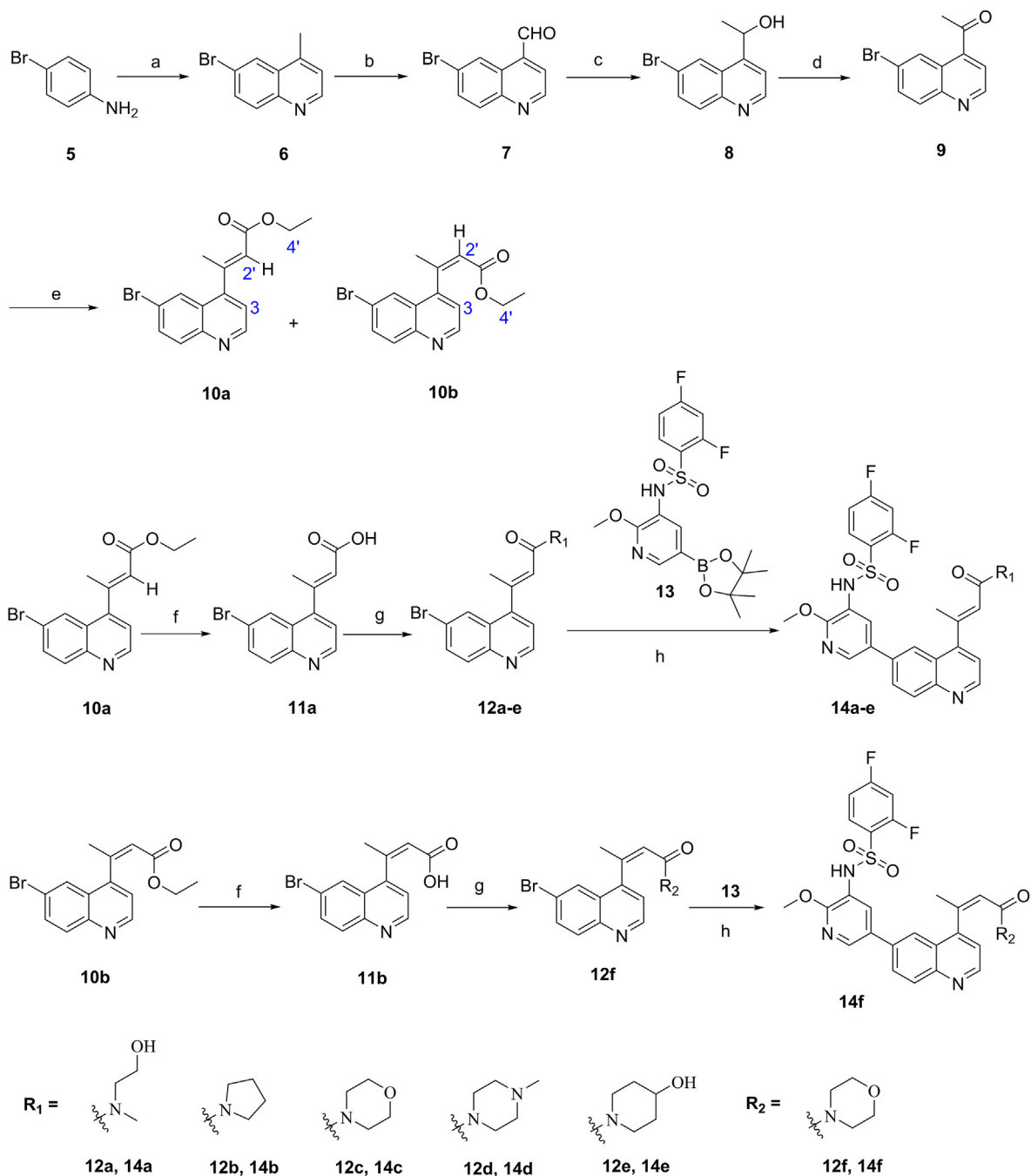


Fig. 2. The design concept of target compounds in this study.



Scheme 1. The synthetic route for target compounds 14a-f. Reagents and conditions: (a) methyl vinyl ketone, FeCl₃, CH₃COOH, 70 °C, 3 h; ZnCl₂, reflux, 2 h; (b) SeO₂, dioxane/H₂O, 100 °C, 2 h; (c) MeMgBr, THF, 0 °C to rt, 12 h; (d) Dess-Martin, NaHCO₃, DCM, 25 °C, 4 h; (e) NaH, triethyl phosphonoacetate, THF, 0 °C to rt, 1.5 h; (f) LiOH·H₂O, THF, 25 °C, 48 h; (g) EDCl, HOBT, CH₂Cl₂, rt, 2 h; amines, triethylamine, 1 h, rt; (h) Pd(dppf)₂Cl₂, K₂CO₃, dioxane/H₂O, 100 °C, 10 h.

Table 1
PI3K α and mTOR inhibitory activities and anti-proliferative activities of compounds **14a-f**.

Compd.	IC ₅₀ (nM)		GI ₅₀ (μ M)	
	PI3K α	mTOR	PC3	U87MG
4	1.04 \pm 0.08	3.2 \pm 0.47	0.45 \pm 0.03	0.22 \pm 0.03
14a	1.5 \pm 0.22	1.7 \pm 0.38	0.29 \pm 0.02	0.38 \pm 0.05
14b	1.2 \pm 0.19	2.1 \pm 0.36	1.16 \pm 0.19	0.39 \pm 0.06
14c	1.1 \pm 0.20	3.3 \pm 0.41	1.67 \pm 0.14	0.61 \pm 0.12
14d	0.80 \pm 0.15	5.0 \pm 0.39	0.36 \pm 0.02	0.14 \pm 0.03
14e	1.4 \pm 0.12	6.1 \pm 0.85	1.08 \pm 0.09	0.60 \pm 0.14
14f	23 \pm 3.3	141 \pm 12	8.02 \pm 0.67	>10.00
GSK2126458	0.30 \pm 0.04	0.34 \pm 0.02	0.25 \pm 0.03	0.22 \pm 0.02

isoforms. Consequently, **14d** displayed potent inhibition against PI3K β , γ , and δ with respective IC₅₀ value of 0.67, 1.3 and 1.3 nM, which suggested that it was a potent pan-class I PI3Ks/mTOR dual inhibitor (Table 2). Considering the different biological functions and the differentiated distribution of the four class I PI3K isoforms, as well as the role played by non-PI3K α isoforms in tumor progress, the pan-class I PI3Ks inhibition was envisioned to improve anti-tumor efficacy and broaden the anti-tumor spectrum.

2.5. Kinase selectivity profiling

To identify its selectivity over the kinases not belonging to PI3K family, compound **14d** was subjected to further profiling against a panel of 52 kinases at the concentration of 10 μ M with DiscoverX's KINOMEScan™ assay (Table 3). The results for primary screen binding interactions were reported as "% Ctrl", and the lower value indicated stronger hits. The results showed that **14d** was highly selective to PI3Ks and PI3K-related kinases, and other lipid kinase, including PIK3CA, PIK3CB, PIK3CD, PIK3CG, MTOR, PIK3C2B, PIK3C2G, PIK4CB, PIP5K2B, VPS34 and PIKFYVE (gene symbol of kinases) (Table 3).

2.6. Western Blot analysis

Subsequently, compound **14d** was evaluated for its capability to down-regulate the levels of some important biomarkers of PAM signaling, including phos-Akt (Ser473), phos-Akt (Thr308), phos-S6 ribosomal protein (Ser235/236) and phos-4E-BP1 (Thr37/46) in U87MG cells with GAPDH introduced as the internal control. The suppressive effect of **14d** was evaluated at the concentrations of 5,

Table 2
Enzymatic activity of compound **14d** against class I PI3Ks.

Compd.	IC ₅₀ (nM)			
	PI3K α	PI3K β	PI3K γ	PI3K δ
14d	0.80 \pm 0.15	0.67 \pm 0.19	1.30 \pm 0.11	1.30 \pm 0.27
GSK2126458	0.30 \pm 0.04	0.19 \pm 0.03	0.44 \pm 0.06	0.78 \pm 0.17

25, 125 and 625 nM. In the Western Blot study, the down-regulation of phos-Akt indicated the suppression of PI3K signaling, while the down-regulation of phos-S6 ribosomal protein and phos-4E-BP1 was the testimony of the ablation of mTOR signaling. Furthermore, the dual suppression of PI3K and mTOR signaling implied the potential to produce synergism and delay the resistance resulted from augmented downstream signaling, as well as S6K/IRS1/PI3K negative feedback loop. According to Fig. 4A, at the concentration as low as 25 nM, **14d** exhibited remarkable suppressive effect on the levels of phos-Akt (Ser473), phos-Akt (Thr308), phos-S6 ribosomal protein (Ser235/236), phos-4E-BP1 (Thr37/46), which was comparable to that of the positive reference GSK2126458 (Fig. 4B). The results demonstrated that compound **14d** can strongly down-regulate the PAM pathway via blocking both PI3K and mTOR signaling, thereby indicating the potential to fulfill synergism and ameliorate the resistance due to PI3K or mTOR mono-inhibition.

2.7. Pharmacokinetic (PK) study

By virtue of its favorable *in vitro* performance, we investigated the PK profiles of **14d** after a PO dose of 5 mg/kg in male SD rats for verifying the contribution of β -methyl group to the improvement in oral exposure (Fig. 5, Table 4). As a result, **14d** exhibited favorable oral exposure (AUC_{0-t} = 1336.16 h \times ng/mL, AUC_{0- ∞} = 1447.63 h \times ng/mL) and high maximum plasma concentration (C_{max} = 903.00 ng/mL). As we anticipated, compound **14d** displayed significantly improved oral exposure in comparison with its β -position-unsubstituted counterpart **4**. It was envisioned the favorable *in vitro* potency and oral exposure of **14d** may translate to the remarkable *in vivo* anti-tumor efficacy.

2.8. *In vivo* anti-tumor efficacy in U87 MG glioblastoma xenograft model

The favorable *in vitro* potency and oral exposure of **14d** prompted us to evaluate its *in vivo* therapeutic efficacy in a U87MG

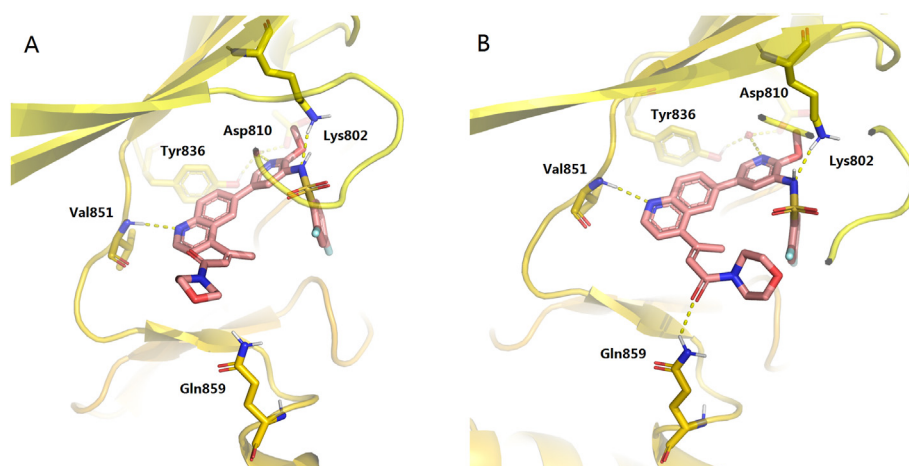


Fig. 3. Docking modes of compounds **14f** and **14c** with PI3K α . (A) The binding mode of **14f** with the catalytic site; (B) the binding mode of **14c** with the catalytic site.

Table 3
Kinase selectivity of **14d** in a panel of kinases (KinomeScan)^a.

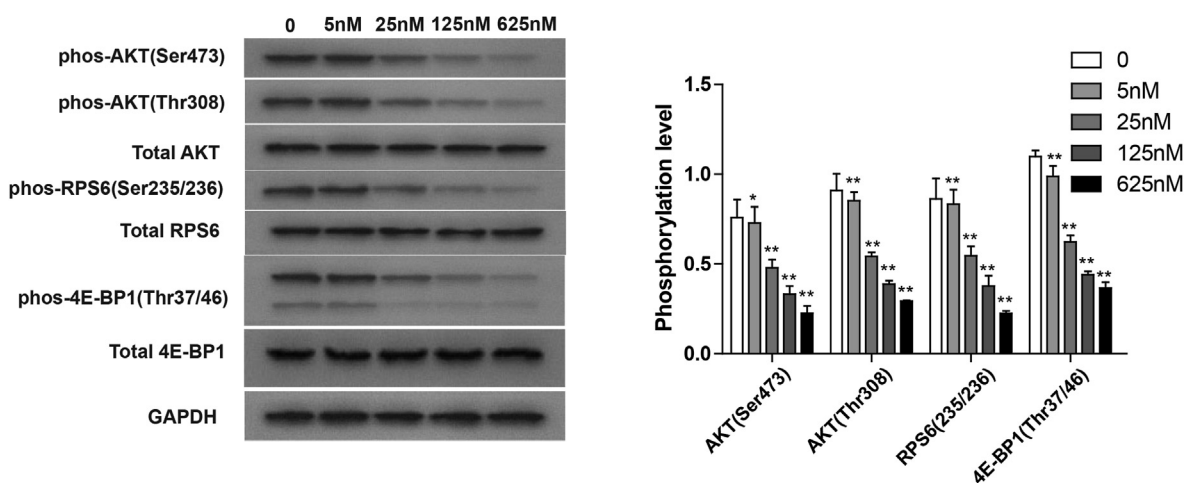
Kinase ^b	% Ctrl ^c								
AAK1	44	CDKL5	69	MAP3K15	45	PIK3C2G	0	PKMYT1	70
ACVR2A	100	CIT	71	MAP3K4	92	PIK3CA	0	PRP4	100
ACVR2B	100	CSNK1A1L	84	MAST1	58	PIK3CB	0	RIPK1	87
ANKK1	100	EPHB6	11	MEK5	63	PIK3CD	0	RIPK4	82
BIKE	49	ERBB3	89	MKK7	73	PIK3CG	0	TIE1	71
BUB1	91	ERK3	78	MTOR	0	PIK4CB	0.55	VPS34	0.1
CDC2L1	93	ERK4	100	NEK10	61	PIKFYVE	1.9	TNNI3K	87
CDK11	95	ERN1	54	PCTK2	100	PIP5K1A	45	YANK1	84
CDK8	96	GAK	22	PCTK3	78	PIP5K1C	35		
CDKL1	82	IRAK3	24	PFTK1	78	PIP5K2B	100		
CDKL3	100	LZK	53	PIK3C2B	0	PIP5K2B	9.4		

^a **14d** against a panel of 52 kinases at the concentration of 10 μM.

^b Gene symbol of kinases.

^c % Ctrl = (tested compound signal - positive control signal)/(negative control signal - positive control signal) × 100, negative control = DMSO (% Ctrl = 100), positive control (% Ctrl = 0).

A



B

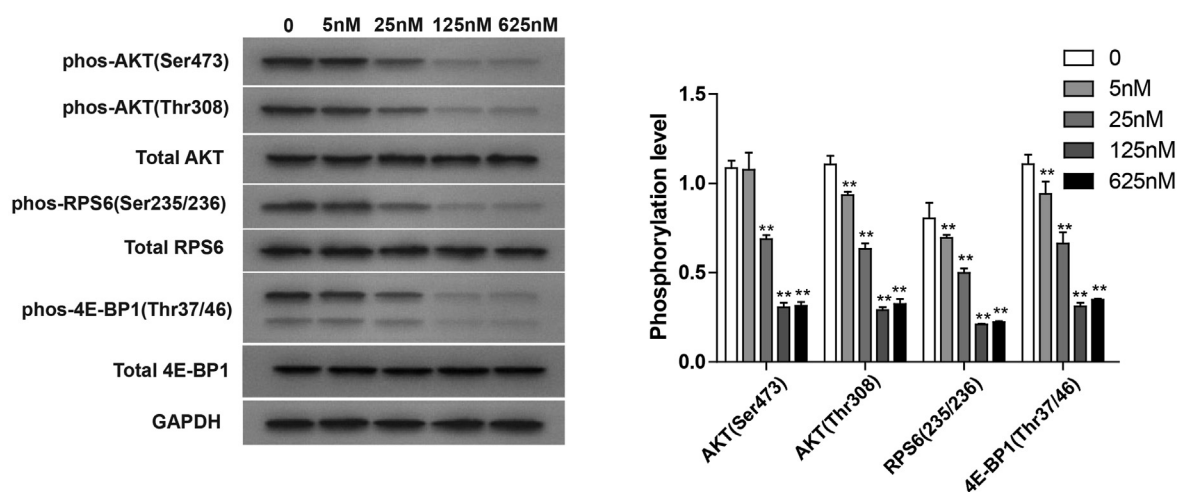


Fig. 4. The suppressive effect of **14d** (A) and GSK2126458 (B) on the phosphorylation of Akt, S6 ribosomal protein and 4E-BP1 in U87MG cells following 3 h treatment: The levels of phos-Akt (Ser473), phos-Akt (Thr308), phos-S6 ribosomal protein (Ser235/236) and phos-4E-BP1 (Thr37/46) in different groups were determined via Western Blot assay. The bar chart represented the quantification of the bands in the Western Blot with the result shown as mean ± SD (n = 3 biological replicates). *p < 0.05, **p < 0.01 V S control (cells incubated without **14d** or GSK2126458).

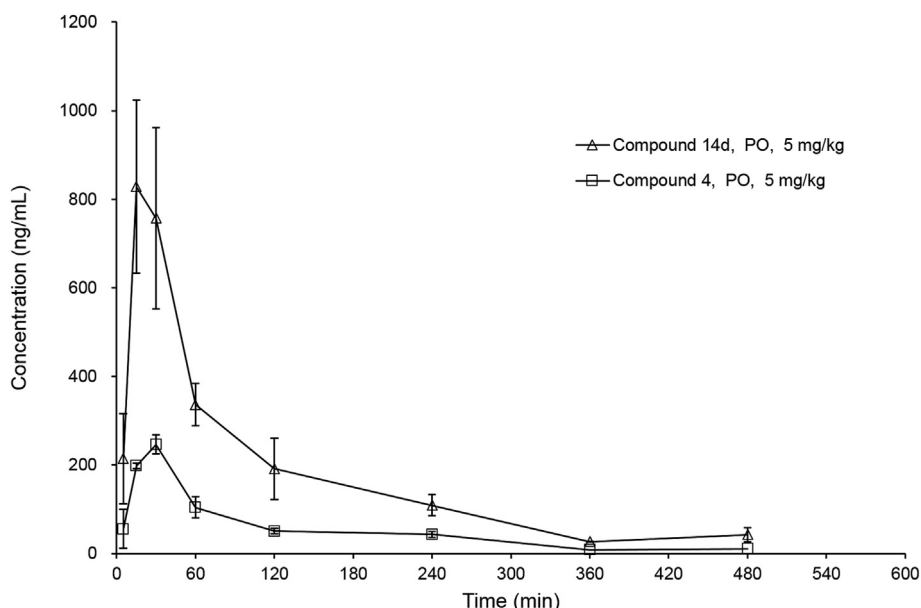


Fig. 5. The concentration-time curves of **14d** and **4** in male SD rats: three animals for PO dose of 5 mg/kg.

Table 4

PK parameters of compounds **4** and **14d**^a.

Compd	$t_{1/2}$ (min)	C_{max} (ng/mL)	AUC_{0-t} (h × ng/mL)	$AUC_{0-\infty}$ (h × ng/mL)	MRT_{0-t} (min)	$MRT_{0-\infty}$ (min)
4	104.09	249.47	379.40	412.31	113.69	155.25
14d	110.75	903.00	1336.16	1447.63	113.79	154.15

^a Mean pharmacokinetic parameters of **4** and **14d** after a PO dose of 5 mg/kg in male Sprague-Dawley rats (n = 3 animals).

glioblastoma xenograft model. Male ICR nude mice were inoculated subcutaneously with U87MG cells to induce solid tumors. After the establishment of the tumors, the mice were randomized and administered upon oral gavage with 30 or 60 mg/kg of **14d** every other day for a period of 24 days. The growth of tumors in individual mice was monitored by measurement of the tumor volume (Fig. 6A) every four days. The results of this study demonstrated that compound **14d** showed a significant inhibition of tumor growth. Tumor growth inhibition of 93.5% was observed at dose of 30 mg/kg. In particular, tumor regression was observed at the dose of 60 mg/kg after this schedule. Furthermore, there was no significant weight loss in the **14d**-treated groups (Fig. 6B).

3. Conclusion

In summary, we described the structural optimization of quinoline analogue **4** to improve its PK properties, particularly the oral exposure. With the strategy of increasing metabolic steric hindrance, β -methyl-4-acrylamido quinoline derivatives **14a-f** were synthesized and biological evaluated. As a result, **14d** showed potent activities in enzymatic assay and anti-proliferative assay, and significantly inhibited PI3K/mTOR signaling at nanomole concentration in Western Blot assay *in vitro*. Further studies indicated that the **14d** showed significantly improved oral exposure in comparison with its β -position-unsubstituted counterpart **4** *in vivo*.

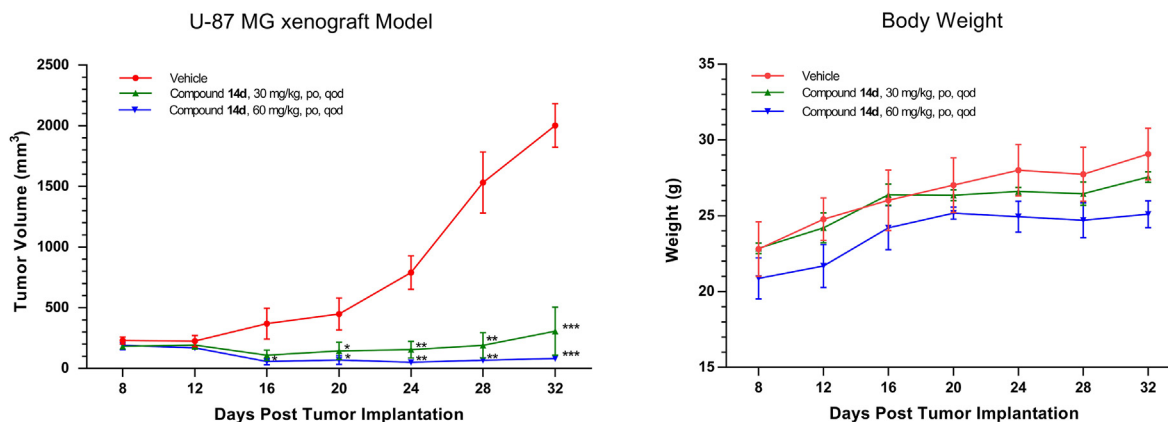


Fig. 6. *In vivo* efficacy of compound **14d**. (A) Tumor volume in a U87 MG glioblastoma xenograft model after treatment with **14d**, symbols represent the mean and standard error, and p-values generated by multiple t tests (*p < 0.05, **p < 0.01, ***p < 0.001 V S vehicle). (B) Bodyweight change in animal treatment with **14d**.

Moreover, **14d** exhibited strong therapeutic efficacy in a U87MG glioblastoma xenograft model *in vivo*. Thus, the strong anti-cancer activities and improved oral exposure suggested that our strategy for structural optimization of quinoline analogue **4** is worthwhile.

4. Experimental section

4.1. Chemistry

¹H and ¹³C NMR spectra were recorded on a Bruker 500 or 400 MHz spectrometer in the indicated solvent with TMS as the internal standard. Chemical shifts and coupling constants (*J*) were given in ppm (δ) and hertz (Hz), respectively. NMR signals were abbreviated as follows: s, singlet; d, doublet; dd, doublet of doublets; t, triplet; td, doublet of triplets; q, quartet; m, multiplet. Signals marked with an asterisk (*) correspond to peaks assigned to the minor rotamer conformation. Mass spectra (MS) were measured on an Esquire-LC-00075 (ESI-MS) spectrometer, while HRMS data were collected by Waters Q-TOF (ESI-MS) Micromass. Column chromatography was performed using silica gel (200–300 mesh, Qingdao haiyang chemical Co., Ltd.). Reagents and solvents were commercially available without further purification.

4.1.1. 6-Bromo-4-methylquinoline (**6**)

To a solution of 4-bromoaniline **5** (33.0 g, 193.02 mmol) in acetic acid (200 mL) was added FeCl₃ (32.0 g, 198.96 mmol) and the mixture was then stirred at room temperature for 10 min. Afterwards, methyl vinyl ketone (17.0 mL, 209.71 mmol) was added dropwise over 30 min and the reaction mixture maintained at 70 °C for 3 h. Then, ZnCl₂ (26.0 g, 194.22 mmol) was added and the solution refluxed for 2 h. After cooling to room temperature, the mixture was evaporated under reduced pressure, basified with NaOH solution (1 N), and extracted with EtOAc. The combined organic extracts were dried over magnesium sulfate and concentrated to give the crude product, which was further purified by column chromatography (20% EA/PE) to give the title intermediate as a brown solid (6.78 g, 30.68 mmol, 16% yield). ¹H NMR (500 MHz, DMSO-*d*₆) δ 8.79 (d, *J* = 4.5 Hz, 1H, Ar-H), 8.29 (d, *J* = 2.0 Hz, 1H, Ar-H), 7.96 (d, *J* = 9.0 Hz, 1H, Ar-H), 7.88 (dd, *J* = 9.0, 2.0 Hz, 1H, Ar-H), 7.43 (d, *J* = 4.5 Hz, 1H, Ar-H), 2.67 (s, 3H, CH₃); ESI-MS: *m/z* = 222.0 [M+H]⁺.

4.1.2. 6-Bromoquinoline-4-carbaldehyde (**7**)

To a solution of 6-bromo-4-methylquinoline (1.0 g, 4.52 mmol) in dioxane/H₂O (V/V, 8/1) was added SeO₂ (2.5 g, 22.34 mmol) at room temperature. After being stirred at 100 °C for 2 h, the reaction mixture was filtered and the solution was dried under reduced pressure. The residue was dissolved in EtOAc and washed successively with saturated aqueous NaHCO₃ and water. The organic phase was then dried over magnesium sulfate and concentrated in vacuo to afford a brown solid, which was purified by column chromatography (20% EA/PE) to give 6-bromoquinoline-4-carbaldehyde (0.78 g, 3.32 mmol, 73%) as a light yellow solid. ¹H NMR (500 MHz, DMSO-*d*₆) δ 10.49 (s, 1H, CHO), 9.28 (d, *J* = 4.5 Hz, 1H, Ar-H), 9.18 (d, *J* = 2.0 Hz, 1H, Ar-H), 8.12 (d, *J* = 9.0 Hz, 1H, Ar-H), 8.11 (d, *J* = 4.5 Hz, 1H, Ar-H), 8.03 (dd, *J* = 9.0, 2.0 Hz, 1H, Ar-H); ESI-MS: *m/z* = 236.0 [M+H]⁺.

4.1.3. 1-(6-bromoquinolin-4-yl)ethan-1-ol (**8**)

To a solution of **7** (30.0 g, 127 mmol) in anhydrous THF (800 mL) was added a solution of MeMgBr in THF (84.8 mL, 3 M) at 0 °C. After the reaction mixture was stirred at room temperature under N₂ atmosphere for 12 h, it was quenched with saturated ammonium chloride solution and extracted with EtOAc (200 mL \times 3). The combined organic layer was dried over anhydrous Na₂SO₄ and

concentrated under reduced pressure. The residue was purified by column chromatography to give the title compound (28.0 g, 111 mmol, 87% yield) as a yellow solid. ¹H NMR (400 MHz, DMSO-*d*₆) δ 8.84 (d, *J* = 4.5 Hz, 1H, Ar-H), 8.37 (d, *J* = 2.0 Hz, 1H, Ar-H), 7.91 (d, *J* = 9.0 Hz, 1H, Ar-H), 7.80 (dd, *J* = 9.0, 2.0 Hz, 1H, Ar-H), 7.57 (d, *J* = 4.5 Hz, 1H, Ar-H), 5.58 (d, *J* = 4.3 Hz, 1H, OH), 5.47–5.31 (m, 1H, CH), 1.39 (d, *J* = 6.5 Hz, 3H, CH₃); ESI-MS: *m/z* = 252.0 [M+H]⁺.

4.1.4. 1-(6-bromoquinolin-4-yl)ethan-1-one (**9**)

To a solution of **8** (28.0 g, 111 mmol) in DCM (500 mL) were added NaHCO₃ (9.33 g, 111 mmol) and Dess-Martin (71.0 g, 166 mmol). After the resultant mixture was stirred at room temperature for 4 h under N₂ atmosphere, the reaction was quenched by sodium sulphite solution. Then, the mixture was extracted with EtOAc (200 mL \times 3), and the organic layer was washed successively with saturated sodium bicarbonate solution (200 mL) and brine (200 mL). The organic phase was dried over anhydrous Na₂SO₄ and concentrated under reduced pressure. The residue was finally purified by column chromatography to give the title compound (20.6 g, 82.7 mmol, 75% yield) as a yellow solid. ¹H NMR (400 MHz, DMSO-*d*₆) δ 9.11 (d, *J* = 4.5 Hz, 1H, Ar-H), 8.65 (d, *J* = 2.0 Hz, 1H, Ar-H), 8.07–8.00 (m, 2H, Ar-H), 7.78 (m, 1H, Ar-H), 2.26 (s, 3H, CH₃); ESI-MS: *m/z* = 250.0 [M+H]⁺.

4.1.5. ethyl 3-(6-bromoquinolin-4-yl)but-2-enoate (**10a**) and ethyl (Z)-3-(6-bromoquinolin-4-yl)but-2-enoate (**10a** and **10b**)

To a suspension of NaH (3.64 g, 152 mmol) in THF was added triethyl phosphonoacetate (42.5 g, 190 mmol, 37.6 mL) at 0 °C, and the resultant mixture was stirred for 30 min at the same temperature. 6-bromoquinoline-4-carbaldehyde (31.6 g, 126 mmol) was then added and the mixture stirred for 1 h at room temperature. The reaction mixture was cooled to 0 °C and ice water was added. After extracting with EtOAc, the organic phase was washed with saturated NaHCO₃ solution, dried over magnesium sulfate, and concentrated in vacuo to afford the crude product, which was further purified by column chromatography to give the title compounds (**10a**: 9.55 g, 29.8 mmol, 24% yield; **10b**: 7.26 g, 22.7 mmol, 18% yield) as yellow solid. **10a**: ¹H NMR (400 MHz, CDCl₃) δ 8.82 (d, *J* = 4.3 Hz, 1H, Ar-H), 7.97–7.91 (m, 2H, Ar-H), 7.73 (dd, *J* = 8.9, 2.1 Hz, 1H, Ar-H), 7.14 (d, *J* = 4.3 Hz, 1H, Ar-H), 5.89 (d, *J* = 1.5 Hz, 1H, alkene hydrogen), 4.21 (q, *J* = 7.1 Hz, 2H, CH₂), 2.51 (d, *J* = 1.5 Hz, 3H, CH₃), 1.28 (t, *J* = 7.1 Hz, 3H, CH₃); ESI-MS: *m/z* = 320.0 [M+H]⁺. **10b**: ¹H NMR (400 MHz, CDCl₃) δ 8.82 (d, *J* = 4.3 Hz, 1H), 7.93 (d, *J* = 8.8 Hz, 1H), 7.81 (d, *J* = 2.0 Hz, 1H), 7.70 (dd, *J* = 8.8, 2.0 Hz, 1H), 7.06 (d, *J* = 4.3 Hz, 1H), 6.16 (d, *J* = 1.5 Hz, 1H, alkene hydrogen), 3.79 (q, *J* = 7.2 Hz, 2H, CH₂), 2.19 (d, *J* = 1.5 Hz, 3H, CH₃), 0.81 (t, *J* = 7.2 Hz, 3H, CH₃); ESI-MS: *m/z* = 320.0 [M+H]⁺.

4.1.6. (E)-3-(6-bromoquinolin-4-yl)but-2-enoic acid (**11a**)

To a solution of **10a** (7.00 g, 21.8 mmol) in THF (20.0 mL) was added a solution of LiOH·H₂O (2.75 g, 65.5 mmol) in H₂O (20.0 mL). After the resultant mixture was stirred at 25 °C for 48 h, the pH was adjusted to 4–5 with 2 N HCl. The precipitate was filtered, washed with water, and dried in vacuo to provide the title intermediate as a white solid (6.00 g, 20.54 mmol, 94% yield). ¹H NMR (400 MHz, DMSO-*d*₆) δ 9.04–8.84 (brs, 1H, Ar-H), 8.81–7.91 (m, 2H, Ar-H), 7.92 (brd, *J* = 8.8 Hz, 1H, Ar-H), 7.46 (brs, 1H, Ar-H), 5.90 (brs, 1H, alkene hydrogen), 2.51 (brs, 3H, CH₃); ESI-MS: *m/z* = 291.8 [M+H]⁺.

4.1.7. (Z)-3-(6-bromoquinolin-4-yl)but-2-enoic acid (**11b**)

This intermediate was prepared from **10b** (7.00 g, 21.8 mmol) according to the synthetic procedure of **11a** as a light yellow solid (5.50 g, 18.8 mmol, 86% yield). ¹H NMR (400 MHz, DMSO-*d*₆) δ 12.12 (brs, 1H, COOH), 8.91 (d, *J* = 4.3 Hz, 1H, Ar-H), 8.0 (d, *J* = 8.8 Hz, 1H,

Ar–H), 7.93–7.86 (m, 2H, Ar–H), 7.34 (d, $J = 4.3$ Hz, 1H, Ar–H), 6.28 (d, $J = 1.5$ Hz, 1H, alkene hydrogen), 2.22 (d, $J = 1.5$ Hz, 3H, CH₃); ESI-MS: $m/z = 291.8$ [M+H]⁺.

4.1.8. General procedure A for the synthesis of intermediates **12a-f**

A solution of **11a** or **11b** (1.0 equiv), EDCI (1.5 equiv) and HOBT (1.5 equiv) in dry CH₂Cl₂ was stirred at room temperature for 2 h. Triethylamine (3.0 equiv) and corresponding amine (2.0 equiv) were then added. After being stirred at room temperature for 1 h, the reaction mixture was washed successively with 1 N NaOH and water. The organic phase was dried with magnesium sulfate and concentrated in vacuo to afford the crude product, which was further purified by silica gel column chromatography to give the desired intermediates. The ¹H NMR and ¹³C NMR spectra of **12a** indicated a mixture of rotamers [34].

4.1.8.1. (*E*)-3-(6-bromoquinolin-4-yl)-*N*-(2-hydroxyethyl)-*N*-methylbut-2-enamide (**12a**). This intermediate was prepared from **11a** (100 mg, 0.34 mmol) and 2-(methylamino)ethan-1-ol (51 mg, 0.68 mmol) according to the general synthetic procedure A as a white solid (85 mg, 0.24 mmol, 71% yield). ¹H NMR (400 MHz, DMSO-*d*₆) δ 8.94/8.93* (2 \times d, $J = 4.4$ Hz, 1H, Ar–H), 8.16/8.12* (2 \times d, $J = 2.0$ Hz, 1H, Ar–H), 8.04*/8.02 (2 \times dd, $J = 8.8, 3.2$ Hz, 1H, Ar–H), 7.96–7.93/7.92–7.89* (2 \times m, 1H, Ar–H), 7.50*/7.48 (2 \times d, $J = 2.0$ Hz, 1H, Ar–H), 6.38/6.30* (2 \times d, $J = 1.2$ Hz, 1H, alkene hydrogen), 4.85/4.76* (2 \times t, $J = 5.2$ Hz, 1H, OH), 3.56 (m, 2H, CH₂), 3.45 (m, 2H, CH₂), 3.10*/2.95 (2 \times s, 3H, CH₃), 2.30–2.22 (m, 3H, CH₃); ¹³C NMR (100 MHz, DMSO-*d*₆) δ 166.50/166.20*, 150.82, 148.90/148.70*, 146.62, 141.41/141.30*, 132.67, 131.87*/131.81, 127.14/126.98*, 126.45, 125.86/125.60*, 120.30*/120.24, 120.12, 58.54*/58.40, 51.85/49.26*, 36.51*/32.66, 20.16/20.08*; ESI-MS: $m/z = 349.0$ [M + H]⁺.

4.1.8.2. (*E*)-3-(6-bromoquinolin-4-yl)-1-(pyrrolidin-1-yl)but-2-en-1-one (**12b**). This intermediate was prepared from **11a** (100 mg, 0.34 mmol) and pyrrolidine (48 mg, 0.68 mmol) according to the general synthetic procedure A as a white solid (89 mg, 0.26 mmol, 76% yield). ¹H NMR (400 MHz, DMSO-*d*₆) δ 8.94 (d, $J = 4.4$ Hz, 1H, Ar–H), 8.12 (d, $J = 2.0$ Hz, 1H, Ar–H), 8.03 (d, $J = 8.8$ Hz, 1H, Ar–H), 7.93 (dd, $J = 8.8, 2.0$ Hz, 1H, Ar–H), 7.49 (d, $J = 4.4$ Hz, 1H, Ar–H), 6.23 (d, $J = 1.2$ Hz, 1H, alkene hydrogen), 3.47 (t, $J = 6.8$ Hz, 2H, CH₂), 3.41 (t, $J = 6.8$ Hz, 2H, CH₂), 2.40 (d, $J = 1.2$ Hz, 3H, CH₃), 1.95–1.77 (m, 4H, CH₂ \times 2); ¹³C NMR (100 MHz, DMSO-*d*₆) δ 164.00, 150.84, 149.07, 146.60, 143.81, 132.69, 131.84, 127.01, 126.26, 124.88, 120.24, 120.14, 46.26, 45.30, 25.61, 23.85, 20.04; MS (ESI) $m/z = 345.1$ [M + H]⁺.

4.1.8.3. (*E*)-3-(6-bromoquinolin-4-yl)-1-morpholinobut-2-en-1-one (**12c**). This intermediate was prepared from **11a** (100 mg, 0.34 mmol) and morpholine (59 mg, 0.68 mmol) according to the general synthesis procedure A as a white solid (93 mg, 0.26 mmol, 76% yield). ¹H NMR (400 MHz, DMSO-*d*₆) δ 8.94 (d, $J = 4.4$ Hz, 1H, Ar–H), 8.08 (d, $J = 2.0$ Hz, 1H, Ar–H), 8.03 (d, $J = 8.8$ Hz, 1H, Ar–H), 7.93 (dd, $J = 8.8, 2.0$ Hz, 1H, Ar–H), 7.51 (d, $J = 4.4$ Hz, 1H, Ar–H), 6.34 (d, $J = 1.2$ Hz, 1H, alkene hydrogen), 3.64–3.52 (m, 8H, CH₂ \times 4), 2.28 (d, $J = 1.2$ Hz, 3H, CH₃); ¹³C NMR (100 MHz, DMSO-*d*₆) δ 164.91, 150.80, 148.54, 146.60, 142.34, 132.66, 131.85, 126.99, 126.35, 124.68, 120.31, 120.12, 66.24, 66.06, 46.09, 41.33, 20.21; ESI-MS: $m/z = 361.0$ [M + H]⁺.

4.1.8.4. (*E*)-3-(6-bromoquinolin-4-yl)-1-(4-methylpiperazin-1-yl)but-2-en-1-one (**12d**). This intermediate was prepared from **11a** (100 mg, 0.34 mmol) and 1-methylpiperazine (68 mg, 0.68 mmol) according to the general synthetic procedure A as a white solid (76 mg, 0.20 mmol, 59% yield). ¹H NMR (400 MHz, DMSO-*d*₆) δ 8.94

(d, $J = 4.4$ Hz, 1H, Ar–H), 8.08 (d, $J = 2.0$ Hz, 1H, Ar–H), 8.03 (d, $J = 8.8$ Hz, 1H, Ar–H), 7.93 (dd, $J = 8.8, 2.2$ Hz, 1H, Ar–H), 7.51 (d, $J = 4.4$ Hz, 1H, Ar–H), 6.33 (d, $J = 1.2$ Hz, 1H, alkene hydrogen), 3.57 (t, $J = 4.4$ Hz, 2H), 3.52 (t, $J = 4.4$ Hz, 2H), 2.37–2.30 (m, 4H), 2.25 (d, $J = 1.2$ Hz, 3H, CH₃), 2.21 (s, 3H, CH₃); ESI-MS: $m/z = 374.1$ [M + H]⁺.

4.1.8.5. (*E*)-3-(6-bromoquinolin-4-yl)-1-(4-hydroxypiperidin-1-yl)but-2-en-1-one (**12e**). This intermediate was prepared from **11a** (100 mg, 0.34 mmol) and 4-hydroxypiperidine (69 mg, 0.68 mmol) according to the general synthetic procedure A as a white solid (88 mg, 0.24 mmol, 71% yield). ¹H NMR (400 MHz, DMSO-*d*₆) δ 8.94 (d, $J = 4.4$ Hz, 1H, Ar–H), 8.08 (d, $J = 2.0$ Hz, 1H, Ar–H), 8.03 (d, $J = 8.8$ Hz, 1H, Ar–H), 7.93 (dd, $J = 8.8, 2.0$ Hz, 1H, Ar–H), 7.51 (d, $J = 4.4$ Hz, 1H, Ar–H), 6.33 (d, $J = 1.2$ Hz, 1H, alkene hydrogen), 4.81 (d, $J = 3.2$ Hz, 1H, OH), 4.08–3.95 (m, 1H, CH), 3.75 (m, 2H, CH₂), 3.30–3.22 (m, 1H, CH₂), 3.19–3.11 (m, 1H, CH₂), 2.23 (d, $J = 1.2$ Hz, 3H, CH₃), 1.77 (m, 2H, CH₂), 1.34 (m, 2H, CH₂); ¹³C NMR (100 MHz, DMSO-*d*₆) δ 164.71, 150.81, 148.50, 146.61, 140.68, 132.62, 131.86, 126.97, 126.44, 125.74, 120.31, 120.07, 65.50, 43.33, 38.44, 34.78, 33.89, 20.11; ESI-MS: $m/z = 375.0$ [M + H]⁺.

4.1.8.6. (*Z*)-3-(6-bromoquinolin-4-yl)-1-morpholinobut-2-en-1-one (**12f**). This intermediate was prepared from **11b** (100 mg, 0.34 mmol) and morpholine (59 mg, 0.68 mmol) according to the general synthetic procedure A as a white solid (89 mg, 0.25 mmol, 74% yield). ¹H NMR (400 MHz, DMSO-*d*₆) δ 8.89 (d, $J = 4.4$ Hz, 1H, Ar–H), 7.98 (d, $J = 8.8$ Hz, 1H, Ar–H), 7.95 (d, $J = 2.0$ Hz, 1H, Ar–H), 7.88 (dd, $J = 8.8, 2.0$ Hz, 1H, Ar–H), 7.36 (d, $J = 4.4$ Hz, 1H, Ar–H), 6.73 (d, $J = 1.2$ Hz, 1H, alkene hydrogen), 3.65–3.51 (m, 4H, CH₂ \times 2), 3.35–3.30 (m, 2H, CH₂), 3.17 (m, 2H, CH₂), 2.22 (d, $J = 1.2$ Hz, 3H, CH₃); ¹³C NMR (100 MHz, DMSO-*d*₆) δ 163.91, 150.63, 148.05, 146.16, 143.26, 132.35, 131.66, 126.90, 126.23, 122.80, 119.73, 119.61, 66.22, 65.98, 45.91, 41.09, 25.71; ESI-MS: $m/z = 361.0$ [M + H]⁺.

4.1.9. General procedure B for the synthesis of target compounds **14a-f**

To a three-neck round bottom flask were added the aryl bromide (1.0 equiv), 2,4-difluoro-*N*-(2-methoxy-5-(4,4,5,5-tetramethyl-1,3,2-dioxaborolan-2-yl)pyridin-3-yl)benzenesulfonamide (**13**) (1.0 equiv), Pd (dppf)₂Cl₂ (0.1 equiv), K₂CO₃ (3.0 equiv) and dioxane/H₂O (V/V, 3/1). The flask was fitted with a N₂ inlet adaptor and purged with N₂ for 15 min. The reaction mixture was then sealed under N₂ atmosphere and stirred at 100 °C for 10 h. After removal of the solvent under reduced pressure, the residue was dissolved in CH₂Cl₂, and the solution was washed with water twice, dried over magnesium sulfate, and concentrated in vacuo. The resultant crude product was purified by column chromatography to yield the desired target compound. The ¹H NMR and ¹³C NMR spectra of **14a** indicated a mixture of rotamers [34].

4.1.9.1. (*E*)-3-(6-(5-((2,4-difluorophenyl)sulfonamido)-6-methoxypyridin-3-yl)quinolin-4-yl)-*N*-(2-hydroxyethyl)-*N*-methylbut-2-enamide (**14a**). The compound was prepared from **12a** (56 mg, 0.16 mmol) and **13** (68 mg, 0.16 mmol) according to the general synthetic procedure B to afford the title compound as an off-white solid (20 mg, 0.035 mmol, 22% yield). ¹H NMR (400 MHz, DMSO-*d*₆) δ 10.38 (s, 1H, NH), 8.91 (d, $J = 4.4$ Hz, 1H, Ar–H), 8.43 (d, $J = 2.1$ Hz, 1H, Ar–H), 8.17 (d, $J = 8.7$ Hz, 1H, Ar–H), 8.12–8.03 (m, 2H, Ar–H), 7.96 (m, 1H, Ar–H), 7.80 (m, 1H, Ar–H), 7.63–7.55 (m, 1H, Ar–H), 7.47*/7.44 (2 \times d, $J = 4.4$ Hz, 1H, Ar–H), 7.23 (m, 1H, Ar–H), 6.43/6.34* (2 \times s, 1H, alkene hydrogen), 4.82/4.76* (2 \times t, $J = 5.3$ Hz, 1H, OH), 3.69*/3.68 (2 \times s, 3H, OCH₃), 3.61–3.44 (m, 4H, CH₂ \times 2), 3.13*/2.96 (2 \times s, 3H, NCH₃), 2.32 (s, 3H, CH₃); ¹³C NMR (100 MHz, DMSO-*d*₆) δ 167.12/166.86*, 165.55 (dd, $J_{C-F} = 250.7$,

12.3 Hz), 159.81 (dd, $J_{C-F} = 255.7, 12.9$ Hz), 158.01/157.99*, 150.94, 150.39/150.16*, 147.89, 143.12/143.05*, 142.63/142.31*, 135.14/135.11*, 134.35/134.21*, 132.33 (d, $J_{C-F} = 10.9$ Hz), 131.01, 129.66/129.63*, 128.90, 125.98/125.88*, 125.83*/125.78, 125.55 (dd, $J_{C-F} = 14.2, 3.8$ Hz), 122.75/122.64*, 120.46, 120.32, 112.38 (dd, $J_{C-F} = 24.7, 2.5$ Hz), 106.31 (t, $J_{C-F} = 26.6$ Hz), 59.04*/58.80, 53.95/52.45*, 49.77, 37.08*/33.08, 20.81/20.71*; HRMS: m/z calcd for $C_{28}H_{27}F_2N_4O_5S$ [M + H]⁺ 569.1670, found 569.1665. HPLC: tR = 7.35 min (97.2% purity).

4.1.9.2. (*E*)-2,4-difluoro-*N*-(2-methoxy-5-(4-(4-oxo-4-(pyrrolidin-1-yl)but-2-en-2-yl)quinolin-6-yl)pyridin-3-yl)benzenesulfonamide (**14b**). The compound was prepared from **12b** (55 mg, 0.16 mmol) and **13** (68 mg, 0.16 mmol) according to the general synthetic procedure B to afford the title compound as an off-white solid (28 mg, 0.050 mmol, 31% yield). ¹H NMR (400 MHz, DMSO-*d*₆) δ 10.40 (s, 1H, NH), 8.91 (d, $J = 3.8$ Hz, 1H, Ar-H), 8.45 (s, 1H, Ar-H), 8.17 (d, $J = 8.7$ Hz, 1H, Ar-H), 8.09 (m, 2H, Ar-H), 7.97 (s, 1H, Ar-H), 7.79 (m, 1H, Ar-H), 7.59 (m, 1H, Ar-H), 7.46 (d, $J = 3.8$ Hz, 1H, Ar-H), 7.24 (m, 1H, Ar-H), 6.29 (s, 1H, alkene hydrogen), 3.69 (s, 3H, OCH₃), 3.54–3.42 (m, 4H, CH₂ × 2), 2.46 (s, 3H, CH₃), 1.86 (m, 4H, CH₂ × 2); ¹³C NMR (100 MHz, DMSO-*d*₆) δ 165.56 (dd, $J_{C-F} = 253.2, 12.1$ Hz), 164.68, 159.82 (dd, $J_{C-F} = 257.5, 13.3$ Hz), 157.95, 150.91, 150.47, 147.91, 144.85, 143.07, 135.13, 134.14, 132.29 (d, $J_{C-F} = 10.8$ Hz), 131.00, 129.56, 128.84, 125.69, 125.56 (dd, $J_{C-F} = 15.8, 3.6$ Hz), 125.07, 122.67, 120.44, 120.41, 112.38 (dd, $J_{C-F} = 22.3, 3.6$ Hz), 106.32 (t, $J_{C-F} = 26.3$ Hz), 53.95, 46.84, 45.81, 26.12, 24.34, 20.70; HRMS: m/z calcd for $C_{29}H_{27}F_2N_4O_4S$ [M + H]⁺ 565.1721, found 565.1709. HPLC: tR = 9.19 min (95.4% purity).

4.1.9.3. (*E*)-2,4-difluoro-*N*-(2-methoxy-5-(4-(4-morpholino-4-oxobut-2-en-2-yl)quinolin-6-yl)pyridin-3-yl)benzenesulfonamide (**14c**). The compound was prepared from **12c** (58 mg, 0.16 mmol) and **13** (68 mg, 0.16 mmol) according to the general synthetic procedure B to afford the title compound as an off-white solid (22 mg, 0.038 mmol, 24% yield). ¹H NMR (400 MHz, DMSO-*d*₆) δ 10.41 (s, 1H, NH), 8.91 (d, $J = 4.4$ Hz, 1H, Ar-H), 8.43 (d, $J = 1.6$ Hz, 1H, Ar-H), 8.17 (d, $J = 8.8$ Hz, 1H, Ar-H), 8.07 (d, $J = 8.8$ Hz, 1H, Ar-H), 8.06 (s, 1H, Ar-H), 7.96 (d, $J = 1.6$ Hz, 1H, Ar-H), 7.79 (m, 1H, Ar-H), 7.59 (m, 1H, Ar-H), 7.48 (d, $J = 4.4$ Hz, 1H, Ar-H), 7.23 (m, 1H, Ar-H), 6.39 (s, 1H, alkene hydrogen), 3.68 (s, 3H, OCH₃), 3.52–3.66 (m, 8H, CH₂ × 4), 2.34 (s, 3H, CH₃); ¹³C NMR (100 MHz, DMSO-*d*₆) δ 165.60, 165.54 (dd, $J_{C-F} = 251.1, 11.9$ Hz), 159.83 (dd, $J_{C-F} = 256.4, 13.3$ Hz), 158.04, 150.89, 149.99, 147.90, 143.32, 143.06, 135.10, 134.29, 132.31 (d, $J_{C-F} = 10.5$ Hz), 131.00, 129.62, 128.84, 125.77, 125.59 (dd, $J_{C-F} = 14.0, 3.1$ Hz), 124.88, 122.69, 120.48, 120.43, 112.36 (dd, $J_{C-F} = 22.2, 3.1$ Hz), 106.30 (t, $J_{C-F} = 26.0$ Hz), 66.74, 66.55, 53.95, 46.64, 41.84, 20.84; HRMS: m/z calcd for $C_{29}H_{27}F_2N_4O_5S$ [M + H]⁺ 581.1670, found 581.1681. HPLC: tR = 8.40 min (95.9% purity).

4.1.9.4. (*E*)-2,4-difluoro-*N*-(2-methoxy-5-(4-(4-methylpiperazin-1-yl)-4-oxobut-2-en-2-yl)quinolin-6-yl)pyridin-3-yl)benzenesulfonamide (**14d**). The compound was prepared from **12d** (60 mg, 0.16 mmol) and **13** (68 mg, 0.16 mmol) according to the general synthetic procedure B to afford the title compound as an off-white solid (25 mg, 0.042 mmol, 26% yield). ¹H NMR (400 MHz, DMSO-*d*₆) δ 8.89 (d, $J = 4.4$ Hz, 1H, Ar-H), 8.26 (d, $J = 2.0$ Hz, 1H, Ar-H), 8.15 (d, $J = 9.4$ Hz, 1H, Ar-H), 8.02 (m, 2H, Ar-H), 7.87 (d, $J = 2.0$ Hz, 1H, Ar-H), 7.80 (m, 1H, Ar-H), 7.54–7.47 (m, 1H, Ar-H), 7.46 (d, $J = 4.4$ Hz, 1H, Ar-H), 7.19 (m, 1H, Ar-H), 6.37 (s, 1H, alkene hydrogen), 3.71 (s, 3H, OCH₃), 3.58 (s, 4H, CH₂ × 2), 2.34 (s, 4H, CH₂ × 2), 2.31 (s, 3H, CH₃), 2.21 (s, 3H, CH₃); ¹³C NMR (100 MHz, DMSO-*d*₆) δ 164.99 (dd, $J_{C-F} = 251.0, 11.6$ Hz), 165.39, 159.75 (d, $J_{C-F} = 255.2, 12.9$ Hz), 157.93, 150.76, 149.93, 147.82, 142.79, 140.35,

135.70, 132.17 (d, $J_{C-F} = 10.3$ Hz), 131.56, 130.93, 129.48, 128.84, 125.81, 125.52 (dd, $J_{C-F} = 14.0, 3.7$ Hz), 125.21, 124.93, 122.43, 120.43, 111.99 (dd, $J_{C-F} = 22.0, 3.4$ Hz), 106.06 (t, $J_{C-F} = 25.9$ Hz), 55.36, 54.76, 53.73, 46.06, 46.03, 41.25, 20.79; HRMS: m/z calcd for $C_{30}H_{30}F_2N_5O_4S$ [M + H]⁺ 594.1986, found 594.2008. HPLC (0.1% TFA): tR = 8.31 min (96.7% purity).

4.1.9.5. (*E*)-2,4-difluoro-*N*-(5-(4-(4-(4-hydroxypiperidin-1-yl)-4-oxobut-2-en-2-yl)quinolin-6-yl)-2-methoxypyridin-3-yl)benzenesulfonamide (**14e**). The compound was prepared from **12e** (60 mg, 0.16 mmol) and **13** (68 mg, 0.16 mmol) according to the general synthetic procedure B to afford the title compound as an off-white solid (18 mg, 0.030 mmol, 19% yield). ¹H NMR (400 MHz, DMSO-*d*₆) δ 10.38 (s, 1H, NH), 8.91 (d, $J = 4.4$ Hz, 1H, Ar-H), 8.41 (d, $J = 2.1$ Hz, 1H, Ar-H), 8.17 (d, $J = 9.4$ Hz, 1H, Ar-H), 8.05 (m, 2H, Ar-H), 7.95 (d, $J = 2.1$ Hz, 1H, Ar-H), 7.80 (m, 1H, Ar-H), 7.59 (m, 1H, Ar-H), 7.48 (d, $J = 4.4$ Hz, 1H, Ar-H), 7.23 (m, 1H, Ar-H), 6.37 (s, 1H, alkene hydrogen), 4.77 (d, $J = 4.0$ Hz, 1H, OH), 4.01 (m, 1H, CH), 3.77 (m, 2H, CH₂), 3.69 (s, 3H, OCH₃), 3.41 (s, 1H, CH₂), 3.17 (m, 1H, CH₂), 2.29 (s, 3H, CH₃), 1.76 (m, 2H, CH₂), 1.42–1.31 (m, 2H, CH₂); ¹³C NMR (100 MHz, DMSO-*d*₆) δ 166.79 (dd, $J_{C-F} = 252.6, 11.4$ Hz), 165.34, 159.82 (dd, $J_{C-F} = 257.2, 13.7$ Hz), 158.01, 150.92, 149.97, 147.90, 142.91, 141.77, 135.13, 134.15, 134.11, 132.32 (d, $J_{C-F} = 10.4$ Hz), 131.02, 129.67, 128.86, 125.91, 125.85, 125.63 (dd, $J_{C-F} = 14.8, 2.6$ Hz), 122.67, 120.52, 112.36 (dd, $J_{C-F} = 22.0, 3.4$ Hz), 106.30 (t, $J_{C-F} = 25.9$ Hz), 65.99, 53.95, 43.83, 38.88, 35.15, 34.38, 20.72; HRMS (ESI) m/z calcd for $C_{30}H_{29}F_2N_4O_5S$ [M + H]⁺ 595.1826, found 595.1823. HPLC: tR = 7.31 min (97.8% purity).

4.1.9.6. (*Z*)-2,4-difluoro-*N*-(2-methoxy-5-(4-(4-morpholino-4-oxobut-2-en-2-yl)quinolin-6-yl)pyridin-3-yl)benzenesulfonamide (**14f**). The compound was prepared from **12f** (58 mg, 0.16 mmol) and **13** (68 mg, 0.16 mmol) according to the general synthetic procedure B to afford the title compound as an off-white solid (20 mg, 0.034 mmol, 21% yield). ¹H NMR (400 MHz, DMSO-*d*₆) δ 10.38 (s, 1H, NH), 8.87 (d, $J = 4.4$ Hz, 1H, Ar-H), 8.45 (s, 1H, Ar-H), 8.12 (d, $J = 8.8$ Hz, 1H, Ar-H), 8.03 (dd, $J = 8.8, 1.6$ Hz, 1H, Ar-H), 7.95 (d, $J = 1.6$ Hz, 1H, Ar-H), 7.92 (d, $J = 1.4$ Hz, 1H, Ar-H), 7.78 (m, 1H, Ar-H), 7.64–7.54 (m, 1H, Ar-H), 7.35 (d, $J = 4.4$ Hz, 1H, Ar-H), 7.23 (td, $J = 8.6, 2.1$ Hz, 1H, Ar-H), 6.67 (s, 1H, alkene hydrogen), 3.69 (s, 3H, OCH₃), 3.47 (s, 2H, CH₂), 3.20 (s, 4H, CH₂ × 2), 3.10 (s, 2H, CH₂), 2.28 (s, 3H, CH₃); ¹³C NMR (100 MHz, DMSO-*d*₆) δ 165.62 (dd, $J_{C-F} = 258.5, 13.2$ Hz), 164.91, 159.84 (dd, $J_{C-F} = 257.4, 14.1$ Hz), 158.05, 150.71, 149.03, 147.49, 143.18, 142.10, 134.62, 134.43, 133.80, 132.27 (d, $J_{C-F} = 10.0$ Hz), 130.76, 129.68, 128.60, 125.65, 125.46 (dd, $J_{C-F} = 12.9, 4.0$ Hz), 123.32, 122.79, 120.06, 112.34 (dd, $J_{C-F} = 19.3, 2.1$ Hz), 106.31 (t, $J_{C-F} = 25.3$ Hz), 66.42, 66.36, 53.91, 46.50, 41.57, 26.21; HRMS: m/z calcd for $C_{29}H_{27}F_2N_4O_5S$ [M + H]⁺ 581.1670, found 581.1678. HPLC: tR = 7.97 min (98.5% purity).

4.2. Biology

4.2.1. In Vitro enzymatic assays, anti-proliferative assays and docking study

The inhibitory activity against class I PI3Ks and mTOR, and the anti-proliferative efficacy against tumor cell lines, as well as the docking study were carried out according to the protocol disclosed in our previous study [35].

4.2.2. KINOMEScan™ assay

Kinase selectivity was screened at the concentration of 10 μM by the KinomeScan binding assay (DiscoverRx) according to a reported protocol [35].

4.2.3. Western Blot assay

The Western blot analysis for evaluating the capability to down-regulate phos-Akt (Ser473), phos-Akt (Thr308), phos-S6 ribosomal protein (Ser235/236), and phos-4E-BP1 (Thr37/46) in U87MG cells was performed according to the protocol disclosed in our previous study with minor modification [35]. The cells were seeded into six-well plate at 1×10^6 cells per well, and then incubated at 37 °C (5% CO₂) overnight prior to drug treatment. Cells were treated with **14d** and GSK2126458 at various concentrations, and incubated at 37 °C for 3 h.

4.2.4. PK study

SD rats were utilized for the PK study of **14d** following oral gavage at the dosage of 5 mg/kg, and the oral dose was formulated in a homogenous opaque suspension of 0.5% methylcellulose. This experiment was performed with the protocol disclosed in our previous work [35]. The study was carried out in accordance with institutional guidelines of the Animal Research Committee at Jiaxing University (log number JXU201850812). The protocol was approved by the institution.

4.2.5. In Vivo therapeutic efficacy against xenograft model

Male ICR nude mice were inoculated subcutaneously with glioblastoma U87MG cells (5×10^6). Once the tumor volume grew to approximately 200 mm³, animals were treated every other day for a period of 24 days upon oral gavage. Tumor volumes and body weights were recorded at intervals of 4 days. Tumor volume was calculated using the following formula: length \times width² \times 0.5 in mm³, and inhibition rate of tumor growth was calculated using the following formula: $100 \times \{1 - [(tumor\ volume_{final} - tumor\ volume_{initial}) / (tumor\ volume_{final} - tumor\ volume_{initial})]\}$ for the vehicle-treated group].

Declaration of competing interest

The authors declare that they have no known competing financial interests or personal relationships that could have appeared to influence the work reported in this paper.

Acknowledgements

The authors thank the project supported by National Natural Science Foundation of China (Grant No. 81903475), the Public Welfare Technology Application Projects of Zhejiang Province (Grant No. 2016C33089) and Jiaxing Public Welfare Research Plan Project (Grant No. 2019AY32007) for financial support.

References

- [1] F. Corti, F. Nichetti, A. Raimondi, M. Niger, N. Prinzi, M. Torchio, E. Tamborini, F. Perrone, G. Pruneri, M. Di Bartolomeo, F. de Braud, S. Pusceddu, Targeting the PI3K/AKT/mTOR pathway in biliary tract cancers: a review of current evidences and future perspectives, *Canc. Treat Rev.* 72 (2019) 45–55.
- [2] F. Barra, G. Evangelisti, L. Ferro Desideri, S. Di Domenico, D. Ferraioli, V.G. Vellone, F. De Cian, S. Ferrero, Investigational PI3K/AKT/mTOR inhibitors in development for endometrial cancer, *Expert Opin. Invest. Drugs* 28 (2019) 131–142.
- [3] D.A. Fruman, H. Chiu, B.D. Hopkins, S. Bagrodia, L.C. Cantley, R.T. Abraham, The PI3K pathway in human disease, *Cell* 170 (2017) 605–635.
- [4] L.M. Thorpe, H. Yuzugullu, J.J. Zhao, PI3K in cancer: divergent roles of isoforms, modes of activation and therapeutic targeting, *Nat. Rev. Canc.* 15 (2015) 7–24.
- [5] A.E. Garces, M.J. Stocks, Class 1 PI3K clinical candidates and recent inhibitor design strategies: a medicinal chemistry perspective, *J. Med. Chem.* 62 (2019) 4815–4850.
- [6] A. Markham, Alpelisib: first global approval, *Drugs* 79 (2019) 1249–1253.
- [7] FDA approves first PI3K inhibitor, *Nat. Rev. Drug Discov.* 13 (2014) 644–645.
- [8] A. Markham, Copanlisib: first global approval, *Drugs* 77 (2017) 2057–2062.
- [9] J.R. Brown, DUO delivers for duvelisib, *Blood* 132 (2018) 2422–2424.
- [10] D. Benjamin, M. Colombi, C. Moroni, M.N. Hall, Rapamycin passes the torch: a new generation of mTOR inhibitors, *Nat. Rev. Drug Discov.* 10 (2011) 868–880.
- [11] L. Lechuga, D.N. Franz, Everolimus as adjunctive therapy for tuberous sclerosis complex-associated partial-onset seizures, *Expert Rev. Neurother.* 19 (2019) 913–925.
- [12] J.A. French, J.A. Lawson, Z. Yapici, H. Ikeda, T. Polster, R. Nabbout, P. Curatolo, P.J. de Vries, D.J. Dlugos, N. Berkowitz, M. Voi, S. Peyrard, D. Pelov, D.N. Franz, Adjunctive everolimus therapy for treatment-resistant focal-onset seizures associated with tuberous sclerosis (EXIST-3): a phase 3, randomised, double-blind, placebo-controlled study, *Lancet* 388 (2016) 2153–2163.
- [13] Z. Jin, H. Niu, X. Wang, L. Zhang, Q. Wang, A. Yang, Preclinical study of CC223 as a potential anti-ovarian cancer agent, *Oncotarget* 8 (2017) 58469–58479.
- [14] E.K. Slotkin, P.P. Patwardhan, S.D. Vasudeva, E. de Stanchina, W.D. Tap, G.K. Schwartz, MLN0128, an ATP-competitive mTOR kinase inhibitor with potent in vitro and in vivo antitumor activity, as potential therapy for bone and soft-tissue sarcoma, *Mol. Canc. Therapeut.* 14 (2015) 395–406.
- [15] K.G. Pike, K. Malagu, M.G. Hummerson, K.A. Menear, H.M. Duggan, S. Gomez, N.M. Martin, L. Ruston, S.L. Pass, M. Pass, Optimization of potent and selective dual mTORC1 and mTORC2 inhibitors: the discovery of AZD8055 and AZD2014, *Bioorg. Med. Chem. Lett.* 23 (2013) 1212–1216.
- [16] D. Rageot, T. Bohnacker, A. Melone, J.B. Langlois, C. Borsari, P. Hillmann, A.M. Sele, F. Beauflis, M. Zvelebil, P. Hebeisen, W. Loscher, J. Burke, D. Fabbro, M.P. Wymann, Discovery and preclinical pharmacological characterization of 5-[4,6-Bis(3-oxa-8-azabicyclo[3.2.1]octan-8-yl))-1,3,5-triazin-2-yl]-4-(difluoro methyl)pyridin-2-amine (PQR620), a highly potent and selective mTORC1/2 inhibitor for cancer and neurological disorders, *J. Med. Chem.* 61 (2018) 10084–10105.
- [17] C. Borsari, D. Rageot, A. Dall'Asen, T. Bohnacker, A. Melone, A.M. Sele, E. Jackson, J.B. Langlois, F. Beauflis, P. Hebeisen, D. Fabbro, P. Hillmann, M.P. Wymann, A conformational restriction strategy for the identification of a highly selective pyrimido-pyrrolo-oxazine mTOR inhibitor, *J. Med. Chem.* 62 (2019) 8609–8630.
- [18] S. Bonazzi, C.P. Gool, A. Gray, N.M. Thomsen, J. Nunez, R.G. Karki, A. Gorde, J.D. Biag, H.A. Malik, Y. Sun, G. Liang, D. Lubicka, S. Salas, N. Labbe-Giguere, E.P. Keane, S. McTighe, S. Liu, L. Deng, G. Piizzi, F. Lombardo, D. Burdette, J.C. Dodart, C.J. Wilson, S. Peukert, D. Curtis, L.G. Hamann, L.O. Murphy, Discovery of a brain-penetrant ATP-competitive inhibitor of the mechanistic target of rapamycin (mTOR) for CNS disorders, *J. Med. Chem.* 63 (2020) 1068–1083.
- [19] C. Borsari, E. Keles, D. Rageot, A. Treyer, T. Bohnacker, L. Bissegger, M. De Pascale, A. Melone, R. Sriramaratnam, F. Beauflis, M. Hamburger, P. Hebeisen, W. Loscher, D. Fabbro, P. Hillmann, M.P. Wymann, 4-(Difluoromethyl)-5-(4-((3R,5S)-3,5-dimethylmorpholino)-6-((R)-3-methylmorpholin-2-yl)-1,3,5-triazin-2-yl)pyridin-2-amine (PQR626), a potent, orally available, and brain-penetrant mTOR inhibitor for the treatment of neurological disorders, *J. Med. Chem.* 63 (2020) 13595–13617.
- [20] S. Crunkhorn, Cancer: combating resistance to EGFR inhibitors, *Nat. Rev. Drug Discov.* 18 (2018) 18.
- [21] H. Daub, K. Specht, A. Ullrich, Strategies to overcome resistance to targeted protein kinase inhibitors, *Nat. Rev. Drug Discov.* 3 (2004) 1001–1010.
- [22] B.D. Hopkins, C. Pauli, X. Du, D.G. Wang, X. Li, D. Wu, S.C. Amadiume, M.D. Goncalves, C. Hodakoski, M.R. Lundquist, R. Bareja, Y. Ma, E.M. Harris, A. Sboner, H. Beltran, M.A. Rubin, S. Mukherjee, L.C. Cantley, Suppression of insulin feedback enhances the efficacy of PI3K inhibitors, *Nature* 560 (2018) 499–503.
- [23] M. Zhan, Y. Deng, L. Zhao, G. Yan, F. Wang, Y. Tian, L. Zhang, H. Jiang, Y. Chen, Design, Synthesis, and biological evaluation of dimorpholine substituted thienopyrimidines as potential class I PI3K/mTOR dual inhibitors, *J. Med. Chem.* 60 (2017) 4023–4035.
- [24] X. Ma, X. Lv, N. Qiu, B. Yang, Q. He, Y. Hu, Discovery of novel quinoline-based mTOR inhibitors via introducing intra-molecular hydrogen bonding scaffold (iMHBS): the design, synthesis and biological evaluation, *Bioorg. Med. Chem.* 23 (2015) 7585–7596.
- [25] S.M. Maira, F. Stauffer, J. Brueggen, P. Furet, C. Schnell, C. Fritsch, S. Brachmann, P. Chene, A. De Pover, K. Schoemaker, D. Fabbro, D. Gabriel, M. Simonen, L. Murphy, P. Finan, W. Sellers, C. Garcia-Echeverria, Identification and characterization of NVP-BE2255, a novel orally available dual phosphatidylinositol 3-kinase/mammalian target of rapamycin inhibitor with potent in vivo antitumor activity, *Mol. Canc. Therapeut.* 7 (2008) 1851–1863.
- [26] K.Y. Chang, S.Y. Tsai, C.M. Wu, C.J. Yen, B.F. Chuang, J.Y. Chang, Novel phosphoinositide 3-kinase/mTOR dual inhibitor, NVP-BGT226, displays potent growth-inhibitory activity against human head and neck cancer cells in vitro and in vivo, *Clin. Canc. Res.* 17 (2011) 7116–7126.
- [27] S.D. Knight, N.D. Adams, J.L. Burgess, A.M. Chaudhari, M.G. Darcy, C.A. Donatelli, J.I. Luengo, K.A. Newlander, C.A. Parrish, L.H. Ridgers, M.A. Sarpong, S.J. Schmidt, G.S. Van Aller, J.D. Carson, M.A. Diamond, P.A. Elkins, C.M. Gardiner, E. Garver, S.A. Gilbert, R.R. Gontarek, J.R. Jackson, K.L. Kershner, L. Luo, K. Raha, C.S. Sherck, C.M. Sung, D. Sutton, P.J. Tummino, R.J. Wegryzn, K.R. Auger, D. Dhanak, Discovery of GSK2126458, a highly potent inhibitor of PI3K and the mammalian target of rapamycin, *ACS Med. Chem. Lett.* 1 (2010) 39–43.
- [28] D.P. Sutherland, L. Bao, M. Berry, G. Castanedo, I. Chuckowree, J. Dotson, A. Folks, L. Friedman, R. Goldsmith, J. Gunzner, T. Heffron, J. Lesnick, C. Lewis, S. Mathieu, J. Murray, J. Nonomiya, J. Pang, N. Pegg, W.W. Prior, L. Rouge, L. Salphati, D. Sampath, Q. Tian, V. Tsui, N.C. Wan, S. Wang, B. Wei, C. Wiesmann, P. Wu, B.Y. Zhu, A. Olivero, Discovery of a potent, selective, and orally available class I phosphatidylinositol 3-kinase (PI3K)/mammalian target

- of rapamycin (mTOR) kinase inhibitor (GDC-0980) for the treatment of cancer, *J. Med. Chem.* 54 (2011) 7579–7587.
- [29] J. Yuan, P.P. Mehta, M.J. Yin, S. Sun, A. Zou, J. Chen, K. Rafidi, Z. Feng, J. Nickel, J. Engebretsen, J. Hallin, A. Blasina, E. Zhang, L. Nguyen, M. Sun, P.K. Vogt, A. McHarg, H. Cheng, J.G. Christensen, J.L. Kan, S. Bagrodia, PF-04691502, a potent and selective oral inhibitor of PI3K and mTOR kinases with antitumor activity, *Mol. Canc. Therapeut.* 10 (2011) 2189–2199.
- [30] F. Beaufils, N. Cmiljanovic, V. Cmiljanovic, T. Bohnacker, A. Melone, R. Marone, E. Jackson, X. Zhang, A. Sele, C. Borsari, J. Mestan, P. Hebeisen, P. Hillmann, B. Giese, M. Zvelebil, D. Fabbro, R.L. Williams, D. Rageot, M.P. Wymann, 5-(4,6-Dimorpholino-1,3,5-triazin-2-yl)-4-(trifluoromethyl)pyridin-2-amine (PQR309), a potent, brain-penetrant, orally bioavailable, pan-class I PI3K/mTOR inhibitor as clinical candidate in oncology, *J. Med. Chem.* 60 (2017) 7524–7538.
- [31] C. Borsari, D. Rageot, F. Beaufils, T. Bohnacker, E. Keles, I. Buslov, A. Melone, A.M. Sele, P. Hebeisen, D. Fabbro, P. Hillmann, M.P. Wymann, Preclinical development of PQR514, a highly potent PI3K inhibitor bearing a difluoromethyl-pyrimidine moiety, *ACS Med. Chem. Lett.* 10 (2019) 1473–1479.
- [32] D. Rageot, T. Bohnacker, E. Keles, J.A. McPhail, R.M. Hoffmann, A. Melone, C. Borsari, R. Sriramaratnam, A.M. Sele, F. Beaufils, P. Hebeisen, D. Fabbro, P. Hillmann, J.E. Burke, M.P. Wymann, (S)-4-(Difluoromethyl)-5-(4-(3-methylmorpholino)-6-morpholino-1,3,5-triazin-2-yl)pyridin-2-amine of class I PI3K and mTOR kinase, *J. Med. Chem.* 62 (2019) 6241–6261.
- [33] X. Ma, L. Shen, J. Zhang, G. Liu, S. Zhan, B. Ding, X. Lv, Novel 4-acrylamido-quinoline derivatives as potent PI3K/mTOR dual inhibitors: the design, synthesis, and in vitro and in vivo biological evaluation, *Front. Chem.* 7 (2019) 236.
- [34] W.E. Stewart, T.H. Siddall, Nuclear magnetic resonance studies of amides, *Chem. Rev.* 70 (1970) 517–551.
- [35] X. Lv, H. Ying, X. Ma, N. Qiu, P. Wu, B. Yang, Y. Hu, Design, synthesis and biological evaluation of novel 4-alkynyl-quinoline derivatives as PI3K/mTOR dual inhibitors, *Eur. J. Med. Chem.* 99 (2015) 36–50.